
COMMENTS AND ADDENDA

The Comments and Addenda section is for short communications which are not of such urgency as to justify publication in *Physical Review Letters* and are not appropriate for regular Articles. It includes only the following types of communications: (1) comments on papers previously published in *The Physical Review* or *Physical Review Letters*; (2) addenda to papers previously published in *The Physical Review* or *Physical Review Letters*, in which the additional information can be presented without the need for writing a complete article. Manuscripts intended for this section may be accompanied by a brief abstract for information-retrieval purposes. Accepted manuscripts will follow the same publication schedule as articles in this journal, and galley proofs will be sent to authors.

Exchange Striction in NiO[†]

L. C. Bartel and B. Morosin

Sandia Laboratories, Albuquerque, New Mexico 87115

(Received 28 September 1970)

Exchange-striction effects have been studied in both the antiferromagnetic and paramagnetic states of NiO. Near-neighbor spin correlation functions as functions of temperature for various choices of J_2/J_1 have been calculated using Green's-function techniques and have been compared with our experimental x-ray data measured between 6 and 698 °K. The temperature dependence of the calculated trigonal distortion using $J_2/J_1=1.5$ yields a good fit with the measurements which vary from 0 at T_N to 4.5' at 0 °K. The isotropic volume contraction (strain) due to the exchange striction is small and never exceeds $\sim 3 \times 10^{-4}$ throughout the temperature range; hence, these latter measurements do not provide detailed information on the correlation functions as was the case for MnO.

The neutron diffraction studies of Shull *et al.*,¹ Roth,^{2,3} and Roth and Slack⁴ have determined that NiO is a type-2 fcc antiferromagnetic (AFM) compound. For this type of AFM ordering, the nearest-neighbor (nn) spins ferromagnetically align if they are on adjacent (111) planes. The next-nearest-neighbor (nnn) spins are also situated on adjacent (111) planes and, hence, are antiferromagnetically aligned. It has also been reported by Roth,^{2,3} Roth and Slack,⁴ Rooksby,⁵ Shimomura *et al.*,⁶ Slack,⁷ and Vernon⁸ that in the paramagnetic state NiO has the fcc NaCl structure and as the temperature is lowered through the Néel temperature (T_N) there is a trigonal distortion of the unit cell. In addition, there is an isotropic volume contraction associated with the magnetic behavior of the material.

In previous papers^{9,10} (hereafter referred to as I and II, respectively), we have studied the experimental and theoretical aspects of the exchange-striction effects in MnO. Much of the theoretical work in II followed closely the work on AFM materials, in particular MnO and α -MnS, of Lines^{11,12} and Lines and Jones.^{13,14} Since a complete temperature study of the exchange-striction effects is lacking for NiO and some of the experimental results of the various investigators are in disagreement,

we have undertaken to study in some detail the exchange-striction effects in NiO in a manner similar to that used in I and II. For experimental and theoretical details, as well as for additional background information, the reader is referred to I and II.

From Eqs. (7) and (8) of II, we see that the trigonal distortion Δ_{eq} and the isotropic lattice contraction $(\delta a/a)_{\text{eq}}$ due to exchange-striction effects are related to the near-neighbor spin correlation functions. In order to calculate these spin correlation functions, it is necessary to determine the nn and nnn exchange constants, J_1 and J_2 .

The calculation of T_N as a function J_1/J_2 using Green's-function techniques in a random-phase approximation is straightforward. From Eq. (2.26) of Ref. 11 we have

$$S(S+1)/3kT_N = \sum_{\vec{k}} A/E_0, \quad (1)$$

where A and E_0 are defined in Ref. 11 as well as in II. In Fig. 1 we show the results of our calculations using Eq. (1) to obtain kT_N/J_2 vs J_1/J_2 for $S=1$.

To calculate J_1 and J_2 for MnO and α -MnS, Lines and Jones^{13,14} used the experimentally observed Curie-Weiss temperature (θ) and the value of the magnetic susceptibility at T_N [$\chi(T_N)$] along with the

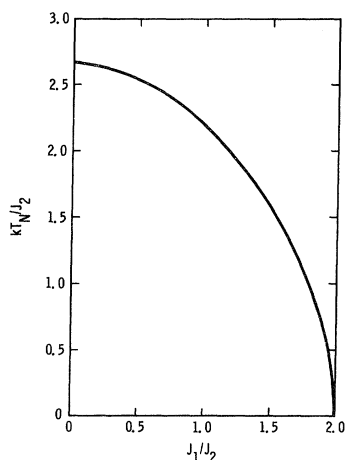


FIG. 1. Calculated Néel temperature T_N for the fcc antiferromagnetic type-2 order vs the ratio of the nn to nnn exchange constants, J_1/J_2 . The calculations were carried out for $S=1$ using the random-phase Green's-function approximation.

calculations of T_N as a function of J_1 and J_2 (similar to our calculations shown in Fig. 1). In using θ to evaluate J_1 and J_2 , it is necessary to extrapolate the $1/\chi$ data from very high temperatures. This requires $\chi(T)$ data for, say, $T \geq 5T_N$. To use $\chi(T_N)$ requires knowing the g factor. In the case of the Mn compounds, $g=2.0$ and there are data for $\chi(T)$ at sufficiently large T so that a meaningful extrapolation of $1/\chi$ can be made.

In the case of NiO, $T_N \approx 523^\circ\text{K}$,¹⁵ and thus it is difficult to obtain $\chi(T)$ at sufficiently large T to ensure an accurate extrapolation to determine θ . Singer¹⁶ has measured $\chi(T)$ for NiO and obtained from the extrapolation of the $1/\chi$ data, $\theta = -2000^\circ\text{K}$, and from the slope of the $1/\chi$ extrapolation he obtained a value of 4.6 for the effective number of Bohr magnetons, which gives $g=3.2$. This value for the g factor is considerably larger than the values $g=2.2$ – 2.3 obtained for Ni^{2+} ions using paramagnetic resonance techniques.¹⁷ In spite of this discrepancy, we shall use Singer's data along with Fig. 1 to obtain J_2 and J_1 . From Eq. (2.3) of Ref. 13 (obtained from Green's-function and molecular-field results), we have $2J_1 + J_2 = k\theta/2S(S+1)$, and using Fig. 1 we obtain $J_1 = 143^\circ\text{K}$, $J_2 = 214^\circ\text{K}$, and $J_2/J_1 = 1.50$. From Eq. (2.4) of Ref. 13 (obtained from Green's-function results), we have $J_2 + J_1 = 12\chi(T_N)/Ng^2\mu_B^2$. Then using Fig. 1, $\chi(T_N) = 11.7 \times 10^{-6}$ emu/g, and $N = 5.43 \times 10^{22}$ cm⁻³ at T_N , we obtain $J_1 = 158^\circ\text{K}$, $J_2 = 218^\circ\text{K}$, and $J_2/J_1 = 1.38$. The fact that these values for the exchange constants agree fairly well is to be expected, since θ and g were obtained from the same set of data. However, using the expressions for $2J_1 + J_2$ and $J_1 + J_2$ and

ignoring the figure, we obtain $J_1 = 125^\circ\text{K}$, $J_2 = 250^\circ\text{K}$, and $J_2/J_1 = 2.00$. Thus there is a large discrepancy between this last determination of J_1 and J_2 and the previous ones; this is anticipated to some extent because of the expected inaccuracies of θ and g determined from the $1/\chi$ extrapolation, as well as inaccuracies of the random-phase approximation in determining kT_N/J_2 as a function of J_1/J_2 .¹⁸

Using Eqs. (18a), (22a), and (22b) of II, we have calculated \bar{S} , $\langle \tilde{S}_i \cdot \tilde{S}_j \rangle_{nn}^b$, $\langle \tilde{S}_i \cdot \tilde{S}_j \rangle_{nnn}^a$, and $\langle \tilde{S}_i \cdot \tilde{S}_j \rangle_{nnn}$ for $J_2/J_1 = 1.35, 1.5$, and 1.7 with $S=1$. We found that as $T \rightarrow 0$, the value of \bar{S} (\bar{S} is the average spin per site) did not vary significantly for these ratios. The values of kT_N/J_2 for $J_2/J_1 = 1.35, 1.5$, and 1.7 are 2.39, 2.44, and 2.49, respectively; thus there is a slight variation of the value of \bar{S} for the three ratios for temperature near T_N . A result similar to that above for \bar{S} was observed for the nn and nnn correlation functions. As a representative value for J_2/J_1 , we have chosen to show the results of the calculations for $J_2/J_1 = 1.5$; thus $J_1 = 143^\circ\text{K}$ and $J_2 = 214^\circ\text{K}$. In Fig. 2 we show the results for \bar{S} , and in Figs. 3 and 4 we show the results of the calculations of the nn and nnn correlation functions, respectively, for $T < T_N$. Since our results for the calculation of the nn and nnn correlation functions for $T > T_N$ agreed to within approximately 2% with those of Lines,¹² the reader is referred to Figs. 7 and 8 of Ref. 12 for the calculation of these correlation functions for $T > T_N$.

A single-crystal (multimagnetic domains) NiO

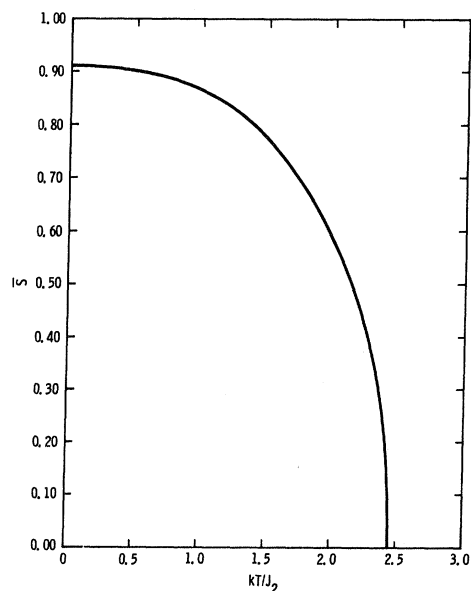


FIG. 2. Calculated average spin per site \bar{S} vs reduced temperature kT/J_2 . The calculations were carried out for $S=1$ and for $J_2/J_1 = 1.5$ using the random-phase Green's-function approximation.

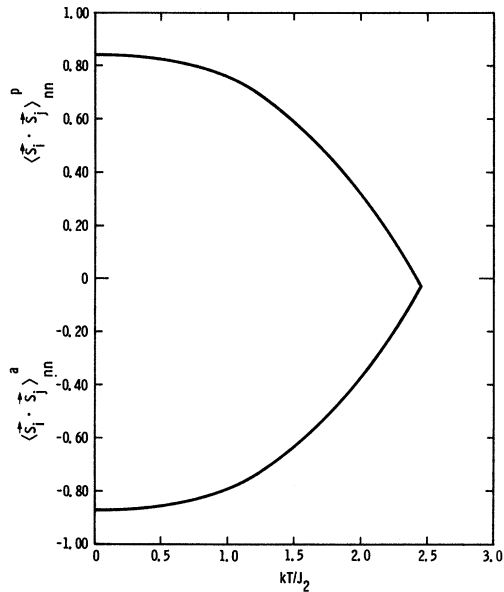


FIG. 3. Calculated nn spin correlation functions for parallel and antiparallel aligned spins vs reduced temperature kT/J_2 ($T \leq T_N$). The calculations were carried out for $S=1$ and for $J_2/J_1=1.5$ using the random-phase Green's-function approximation.

sample, grown by the vapor deposition process with NiCl_2 as the transporting media, was obtained from Professor D. R. Winder, Colorado State University. Experimental procedures are described in I; above

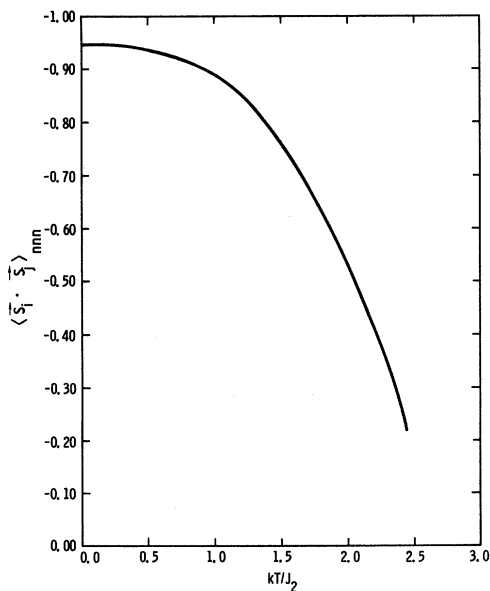


FIG. 4. Calculated nnn spin correlation function vs reduced temperature kT/J_2 ($T \leq T_N$). The calculations were carried out for $S=1$ and for $J_2/J_1=1.5$ using the random-phase Green's-function approximation.

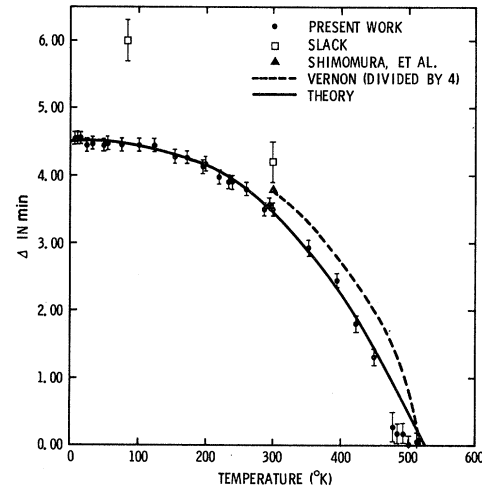


FIG. 5. Angle Δ of the pseudocubic cell, $\alpha = \frac{1}{2}\pi + \Delta$, for NiO below T_N . The experimentally determined angles of this work are shown, as well as the work of Slack (Ref. 7), Shimomura *et al.* (Ref. 6), and Vernon (Ref. 8); Rooksby's (Ref. 5) room-temperature value was the same as our value. The solid curve is the calculated angle [Eq. (7a) of II] normalized to the experimental curve at $T=0^\circ\text{K}$.

room temperature, a new high-temperature single-crystal furnace¹⁹ replaced the low-temperature Dewar. The trigonal distortion and lattice constant as functions of temperature were measured for our sample from 6 to 698 °K. As in I, we are employing the pseudocubic cell (4 times the volume of the primitive cell) with cell edge a_0 and angle α ; here $\alpha = \frac{1}{2}\pi + \Delta$, where Δ , the trigonal distortion, is a small angle. These results are shown in Figs. 5 and 6. We have determined that the trigonal distortion and lattice constant for NiO as $T \rightarrow 0^\circ\text{K}$ are $4.5'$ (1.3×10^{-3} rad) and 4.1705 \AA , respectively. Values for the trigonal distortion as $T \rightarrow 0$ obtained by Rooksby⁵ and Slack⁷ are $11'$ and $6'$, respectively. Our room-temperature value for the trigonal distortion is $3.5'$ to be compared to the values $3.5'$, $3.8'$, $4.2'$, and $3.8'$ obtained by Rooksby,⁵ Shimomura *et al.*,⁶ Slack,⁷ and Vernon.^{8,20} The variation in the values for the trigonal distortion, in excess of experimental error, may be due to impurities in the NiO,²¹ or to an excess of oxygen.^{6,22} To check this assertion we measured a_0 (298 °K) in powder and ground single-crystal samples of NiO obtained from several different sources. We found differences of the order of our standard deviation (0.0003 \AA) in a_0 from sample to sample. For our single-crystal sample, a_0 (298 °K) was 4.1759 \AA in excellent agreement with the value of Shimomura *et al.*⁶ of 4.1758 \AA for stoichiometric NiO. They showed that with excess oxygen the trigonal distortion decreases while a_0 increases. Unfortunately our samples were not of sufficient quantity to do a definitive

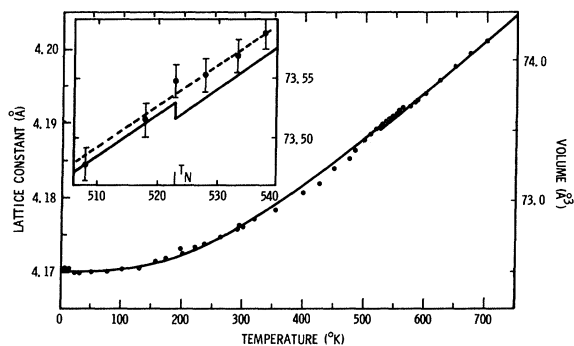


FIG. 6. Lattice constants (or volume) for NiO between 7 and 700 °K. The solid curves are the calculated lattice constants vs temperature, including the magnetic contribution [Eq. (8a) of II], with $J_2\epsilon_2 = 60$ °K (Ref. 24), a Debye temperature of 900 °K, and a linear thermal expansion coefficient of $7.93 \times 10^{-6} \text{ deg}^{-1}$. A curve for a corresponding solid ignoring the magnetic interactions would be slightly above (but within a linewidth of) the shown solid curve. Values of this absent curve are $+0.0187 \text{ \AA}^3$ above the shown curve at 7 °K, as indicated in the inset at T_N , and $+0.0190$ at 700 °K. Errors in the measurements are approximately the size of the data points. In the insert, the solid curve are the calculated lattice constants with the magnetic contribution and the dashed line are the calculations without the magnetic contribution.

chemical analysis as did Shimomura *et al.*⁶; however, our good agreement with respect to a_0 suggests that only very small amounts of impurities or differences in oxygen content are present in our samples.

Using the values for the nn correlation functions given in Fig. 3, we obtain $S^2 = 1.713$ as $T \rightarrow 0$ °K, and using the elastic constants,²³ $N = 5.52 \times 10^{22} \text{ cm}^{-3}$, and $\Delta_{\text{eq}} = 1.3 \times 10^{-3}$ as $T \rightarrow 0$ °K, we obtain $J_1\epsilon_1 = 190$ °K from Eq. (7a) of II. Thus for $J_2 = 214$ °K we obtain from Eq. (10a) of II, $j/J_2 = 0.0007$. For this value of j/J_2 we found that the values for \bar{S} and the correlation function varied insignificantly from those values for $j/J_2 = 0$. Thus, the correlation functions and \bar{S} for NiO are not affected so much by the trigonal distortion as for MnO. Primarily this is because we have $S = \frac{5}{2}$ for MnO and $S = 1$ for NiO, so that at a given temperature \bar{S} and hence S^2 will be larger for MnO than for NiO. In addition the nn and nnn correlation functions are smaller for NiO than for MnO, and so $(\delta a/a)_{\text{eq}}$ [Eq. (8) of II] would have even less of an effect on the detailed shapes of \bar{S} and the correlation function curves than it does for MnO.

Using the calculated nn correlation functions (Fig. 3), we have calculated the normalized trigonal distortion which is proportional to $S^2 = \langle \vec{S}_i \cdot \vec{S}_j \rangle_{\text{nn}}^b - \langle \vec{S}_i \cdot \vec{S}_j \rangle_{\text{nn}}^a$. The solid line in Fig. 5 is the result of our calculations. It is noteworthy that the normalized curves when $J_2/J_1 = 1.35$ or 1.7 are essentially the same as the curve for $J_2/J_1 = 1.5$ shown

in Fig. 5. Calculations for $J_2/J_1 = 0.6$ or 1.0 give somewhat flatter curves than those for $J_2/J_1 > 1.35$, with the curve for $J_2/J_1 = 0.6$ yielding the lesser curvature.

The magnetic contribution to the lattice strain, $(\delta a/a)_{\text{eq}}$, depends on the correlation functions $\langle \vec{S}_i \cdot \vec{S}_j \rangle_{\text{nnn}}$ and $\mathcal{R}^2 = \langle \vec{S}_i \cdot \vec{S}_j \rangle_{\text{nn}}^b + \langle \vec{S}_i \cdot \vec{S}_j \rangle_{\text{nn}}^a$, Eq. (8) of II. For $T < T_N$, \mathcal{R}^2 is small because of the partial cancellation of the terms. However, for $T > T_N$, the contribution to $(\delta a/a)_{\text{eq}}$ proportional to \mathcal{R}^2 can be approximately 30% of the contribution proportional to $\langle \vec{S}_i \cdot \vec{S}_j \rangle_{\text{nnn}}$. In considering the magnetic contribution to the lattice strain, we will not ignore those terms proportional to \mathcal{R}^2 . In a manner similar to that outlined in I, we attempted a least-squares fitting procedure to the lattice constant which accounts for the normal thermal expansion effects and the magnetic contribution. Using a value of $J_2\epsilon_2 \sim 60$ °K as suggested by our data,²⁴ the solid curve in Fig. 6, which includes the magnetic contribution, is obtained for the calculated lattice constant as a function of temperature. (The calculated lattice constant ignoring the magnetic contribution would be approximately a linewidth larger in volume than the solid curve shown in Fig. 6.) Our data are consistent with a higher Debye temperature (900 °K) than would be obtained from the Lindemann relation⁹ (~ 500 °K). Our high-temperature data yield a linear thermal expansion coefficient of $7.93 \times 10^{-6} \text{ deg}^{-1}$. As we can see from Fig. 6, the magnetic contribution to the lattice constant is small for NiO, and a reasonable fit to the data can be made ignoring the magnetic contribution.

We now wish to compare the effect of crystalline anisotropy in NiO with the effect in MnO where it is believed to be small.¹³ Lines and Jones¹³ have discussed the effects of effective anisotropy fields for MnO. From the Eqs. (4.22) and (4.2) of Ref. 13 we can calculate the "out-of-plane" anisotropy parameters K_1 and D_1 . The "in-plane" anisotropy constant D_2 is believed to be considerably smaller than D_1 .^{13,25} Using the AFM resonance of 52.48 °K²⁶ and $\chi_1(T=0) = 7.9 \times 10^{-6} \text{ emu/g}$,¹⁶ we obtain for NiO $K_1 = 0.11 \times 10^7 \text{ erg cm}^{-3}$ and $D_1 = 0.21$ °K. For MnO, $K_1 = 1.16 \times 10^7 \text{ erg cm}^{-3}$ and $D_1 = 0.44$ °K.¹³ Thus for NiO with its rather large exchange energy, the crystalline anisotropy energy appears to be less important than for MnO. The experimentally observed single-axis spin structure for NiO^{4,13} confirms our belief that the crystalline anisotropy energy is small, and the dominant effect is the isotropic exchange energy. Recently White *et al.*²⁷ have determined the in-plane anisotropy field to be approximately 0.1 Oe. The equivalent anisotropy field for the out-of-plane anisotropy determined above would be 610 Oe. Thus the in-plane anisotropy is indeed very much smaller than the out-of-plane anisotropy as asserted above.

[†]Work supported by the U. S. Atomic Energy Commission.

¹C. G. Shull, W. A. Strauser, and E. O. Wollan, *Phys. Rev.* **83**, 333 (1951).

²W. L. Roth, *Phys. Rev.* **110**, 1333 (1958).

³W. L. Roth, *Phys. Rev.* **111**, 772 (1958).

⁴W. L. Roth and G. A. Slack, *J. Appl. Phys.* **31**, 352S (1960).

⁵H. P. Rooksby, *Acta Cryst.* **1**, 226 (1948).

⁶Y. Shimomura, I. Tsubokawa, and M. Kojima, *J. Phys. Soc. Japan* **9**, 521 (1954).

⁷G. A. Slack, *J. Appl. Phys.* **31**, 1571 (1960).

⁸M. W. Vernon, *Phys. Status Solidi* **37**, K1 (1970).

⁹B. Morosin, *Phys. Rev. B* **1**, 236 (1970) (referred to as I).

¹⁰L. C. Bartel, *Phys. Rev. B* **1**, 1254 (1970) (referred to as II).

¹¹M. E. Lines, *Phys. Rev.* **135**, A1336 (1964).

¹²M. E. Lines, *Phys. Rev.* **139**, A1304 (1965).

¹³M. E. Lines and E. D. Jones, *Phys. Rev.* **139**, A1313 (1965).

¹⁴M. E. Lines and E. D. Jones, *Phys. Rev.* **141**, 525 (1966).

¹⁵M. Föex, *Compt. Rend.* **227**, 193 (1948); J. R. Tomlinson, L. Domash, R. G. Hay, and C. W. Montgomery, *J. Am. Chem. Soc.* **77**, 909 (1955).

¹⁶J. R. Singer, *Phys. Rev.* **104**, 929 (1956).

¹⁷W. Low and R. S. Rubins, in *Paramagnetic Resonance*, edited by W. Low (Academic, New York, 1963), Vol. I, p. 84.

¹⁸An alternative method of determining J_1 and J_2 would be to use molecular-field theories. From Eqs. (7.22), (8.7), and (8.12) in J. S. Smart [*Effective Field Theories of Magnetism* (Saunders, Philadelphia, 1966), pp. 58–85], we calculate for NiO $J_1=98^\circ\text{K}$ and $J_2=131^\circ\text{K}$ giving $J_2/J_1=1.33$ (note the factor 2 in the definition of J_1 and J_2 , i.e., our J 's are 2 times Smart's J 's). D. H. Martin [*Magnetism in Solids* (MIT Press, Cambridge, Mass., 1967), p. 358] has calculated $J_1=100^\circ\text{K}$ and $J_2=170^\circ\text{K}$

(again note the factor of 2) which gives a ratio of $J_2/J_1=1.7$. However, we should be very careful in taking the molecular-field determinations of the exchange constants too seriously. The molecular-field determinations give results for MnO which are in complete disagreement with the Green's-function results of Lines and Jones (Ref. 13). The exchange constants determined by Lines and Jones appear to fit the wide variety of experimental data.

¹⁹R. W. Lynch and B. Morosin, *J. Appl. Cryst.* (to be published).

²⁰The values for the distortion obtained by Vernon, Ref. 8, were divided by 4 for a comparison.

²¹Y. Shimomura and I. Tsubokawa, *J. Phys. Soc. Japan* **9**, 19 (1954).

²²D. P. Bogatskii, *Zh. Obshch. Khim.* **21**, 3 (1951).

²³I. Wakabayashi, H. Kobayashi, H. Nagasaki, and S. Minomura [*J. Phys. Soc. Japan* **25**, 227 (1968)] have measured the compressibility (κ) for NiO ($\kappa_{\text{NiO}}=5.4\times 10^{-7}$ bar⁻¹), and hence, assuming cubic symmetry, we have $C_{11}+2C_{12}$ since $\kappa=3/(C_{11}+2C_{12})$. Using the elastic constants for MnO [D. W. Oliver, *J. Appl. Phys.* **40**, 893 (1969)], we calculate $\kappa_{\text{MnO}}=6.48\times 10^{-7}$ bar⁻¹.

Now assuming the elastic constants for NiO and MnO scale as the compressibilities, we have for NiO $C_{11}=2.7\times 10^{12}$ dyn cm⁻², $C_{12}=1.4\times 10^{12}$ dyn cm⁻², and $C_{44}=0.95\times 10^{12}$ dyn cm⁻².

²⁴Since the magnetic contribution to the isotropic volume contraction is small for NiO (Fig. 6), it is difficult to accurately determine a value for $J_2\epsilon_2$ from our lattice constant data. After several trials using various values of $J_2\epsilon_2$, we found that $J_2\epsilon_2=60^\circ\text{K}$ gave a reasonable fit to the experimental data.

²⁵F. Keffer and W. O'Sullivan, *Phys. Rev.* **108**, 637 (1957).

²⁶J. A. Reissland and N. A. Begum, *J. Phys. C* **2**, 874 (1969).

²⁷H. W. White, J. W. Battles, and G. E. Everett, *Solid State Commun.* **8**, 313 (1970).

Current-Induced Intermediate State in Type-1 Superconductors

D. C. Baird

Department of Physics, Royal Military College, Kingston, Ontario, Canada

and

B. K. Mukherjee*

School of Physical Sciences, University of St. Andrews, St. Andrews, Fife, Scotland

(Received 23 July 1970)

We have improved our previous model of the intermediate state in type-1 current-carrying superconductors. In addition to predicting a resistance transition in reasonable agreement with experimental observations, the model gives good agreement with experimental values for the radius of the intermediate-state core as obtained by Rinderer.

In a previous paper¹ (referred to hereafter as BM) we presented a model of the intermediate state in current-carrying type-1 superconductors. The main theoretical criterion used was that, at equilibrium, the magnetic field H at all points on a nor-

mal-superconducting boundary should have the critical value H_c . Ideally the field should also be H_c throughout the whole normal region, but it is not possible to find a finite structure to satisfy this ideal condition. Supercooling is therefore involved, since